

Transmission Electron Microscopy with *in situ* Ion Irradiation

J.A. Hinks

*School of Computing and Engineering, University of Huddersfield, Queensgate, Huddersfield, HD1 3DH,
United Kingdom*

j.a.hinks@hud.ac.uk

Abstract

The macroscopic properties of materials exposed to irradiation are determined by radiation damage effects which occur on the nanoscale. These phenomena are complex dynamic processes in which many competing mechanisms contribute to the evolution of the microstructure and thus to its end-state. In order to explore and understand the behaviour of existing materials and to develop new technologies, it is highly advantageous to be able to observe the microstructural effects of irradiation as they occur.

Transmission electron microscopy with *in situ* ion irradiation is ideally suited to this kind of study. This review focuses on some of the important factors in designing this type of experiment including sample preparation and ion beam selection. Also presented are a brief history of the development of this technique and an overview of the instruments in operation today including the latest additions.

Keywords: Transmission electron microscopy (TEM); ion-solid interactions; radiation effects

Introduction

Transmission electron microscopy (TEM) with *in situ* ion irradiation can give invaluable insights into the response of materials to radiation. Traditional *ex situ* studies are inevitably limited to the study of end states and thus are unable to capture the dynamic evolution of microstructures. Although multiple irradiation steps can be performed with transfer to another instrument for characterisation after each step, this process can be time consuming and the number of steps limited by the fragility and/or contamination of the sample. Furthermore, it can be problematic to maintain the same experimental conditions such as temperature throughout irradiation, transfer and observation. In the case of a TEM sample it can be difficult to return to exactly the same nanosized region especially given the morphological changes which can occur under irradiation. However, TEM with *in situ* ion irradiation can overcome these challenges by constantly following the same region of a sample from virgin to end-fluence whilst controlling variables such as temperature and minimising the risks incurred during sample transfer.

In 1961, the creation of black-spot damage in gold samples under TEM observation was reported by Pashley and Presland [1] working at the Tube Investment Laboratories, Cambridge (UK). They suspected these could “*arise from bombardment by energetic negative ions emitted from the tungsten filament of the electron gun*” [1]. To rule out electron beam effects they used deflection coils mounted above the sample position in their Siemens Elmiskop I 100 kV TEM as a mass-selector to deflect the electrons away from the sample whilst not causing significant deviation of any ions. After an hour with the electron beam and coils turned on, a previously-virgin sample was found to contain the same black-spot damage despite the electron beam having been deflected away by the coils. In another test, two gold samples were loaded above and below each other such that ions would be stopped in the top foil but with electrons able to pass through both foils. The objective lens could be used to form a TEM image of either the top or bottom sample. The radiation damage was observed in the top sample with very little in the bottom sample. Pashley and Presland concluded that the “*direct observation of ion damage in the electron microscope thus represents a powerful means of studying radiation damage*” [1] and the technique of TEM with *in situ* ion irradiation was born.

The story now moves to Canada and the Chalk River Nuclear Laboratories in the mid-1960s. Howe *et al.* [2]–[5] used another Siemens Elmiskop I with an electron filament coated so as to enhance the flux of O^- ions. Their experiments on radiation damage in copper, gold and aluminium below 30 K were also the first experiments to combine low temperature and ion irradiation with *in situ* TEM. In another first, a Faraday cup was installed to allow measurement of the ion beam flux within the microscope column [4].

Later in the same decade came the first TEM to be interfaced with an external ion-accelerator in the laboratories of the Atomic Energy Research Establishment at Harwell (UK) [6], [7]. This instrument consisted of a JEOL JEM-6A connected to a 120 kV heavy-ion accelerator and featured electrostatic deflection on the outside of the TEM column to achieve an angle of 35° between the electron and ion beams. This facility was later upgraded to JEOL JEM-200A in the early 1970s [8].

Further systems were developed throughout the 1970s, including at the University of Virginia (USA) [9], the Centre de Sciences Nucléaires et de Sciences de la Matière (CSNSM) Orsay (France) [10] and the University of Tokyo (Japan) [11]. In the 1980s and 1990s, there followed several facilities such as: the High Voltage Electron Microscope (HVEM) [12], [13] and Intermediate Voltage Electron Microscope (IVEM) [14] both at Argonne National Laboratory (USA); the JEOL JEM-ARM1000 at the National Institute for Materials Science (NIMS) [15] and JEOL JEM-ARM1300 at Hokkaido University [16] (both Japan); and more recently, the Joint Accelerators for Nano-science and Nuclear Simulation (JANNuS) facility at CSNSM Orsay (France) [17], the Microscope and Ion Accelerator for Materials Investigations (MIAMI) facility at the University of Huddersfield (UK) [18] and the I³TEM facility at the Ion Beam Laboratory at Sandia National Laboratories (USA) [19]. The interested reader is directed to previous reviews on the technique of TEM with *in situ* ion irradiation [16], [20]–[26].

Ion beam selection

The choice of ion species and energy for an *in situ* TEM experiment needs to be made with attention paid to sample thickness, orientation and composition as well as the phenomena to be investigated. Figure 1a shows the results of calculations performed using the *Stopping Range of Ions in Matter* (SRIM 2013)

Monte Carlo computer program [27] for helium irradiation of a selection of nuclear materials at normal incidence for a range of typical TEM sample thicknesses, d , from 10 to 100 nm. To achieve a projected range, R_p , in the middle of a sample (i.e. $R_p = 0.5d$) to study, for example, helium accumulation in these materials requires just 3.3 keV for a 50 nm sample of silicon carbide but 16.8 keV for 100 nm of tungsten.

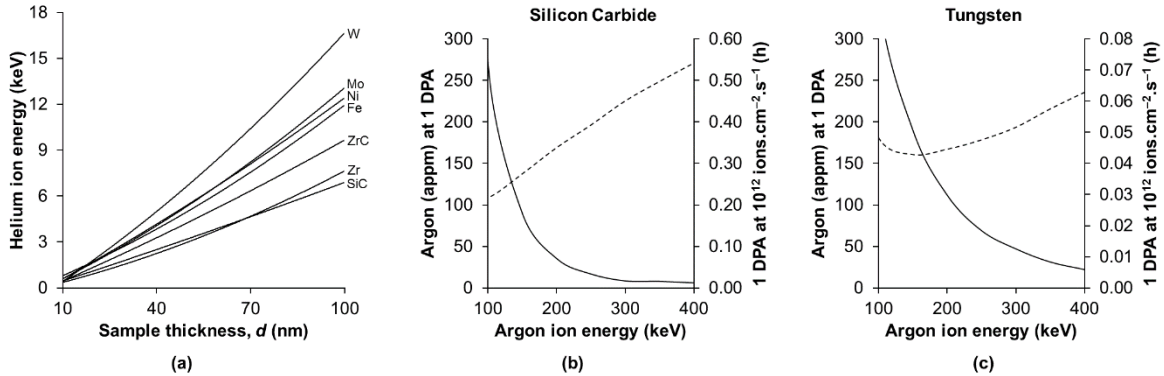


Figure 1: Results of SRIM [27] calculations for: (a) the helium ion energy required to achieve a projected range in the middle of a sample of various nuclear materials; and the amount of implanted argon (solid lines) and irradiation time (dashed lines) for 1 DPA with a flux of 10^{12} ions. $\text{cm}^{-2}\cdot\text{s}^{-1}$ in a 50 nm sample of (b) silicon carbide and (c) tungsten illustrating how higher energies can be used to minimise implantation in a TEM sample when investigating the effects of atomic displacements but at the cost of increased irradiation times. Note the order of magnitude difference in the irradiation times between (b) and (c).

Where the purpose of the experiment is to explore the accumulation of atomic displacements (measured in Displacements Per Atom (DPA)) then heavy inert gas ions or self-ions can be used. (At 1 DPA every atom in the target has, on average, been displaced once from its lattice site.) However, when irradiating to high levels of DPA, the amount of implanted gas or additional interstitial atoms should be considered as these can become significant factors. Figures 1b and 1c show the Atomic Parts Per Million (APPM) per DPA which would be introduced into a 50 nm target in the cases of silicon carbide (low Z) and tungsten (high Z) for a range of argon ion energies. As can be seen, the amount of implanted gas can

be minimised by using higher energy ions which are more likely to travel all the way through a thin TEM sample. However, this can result in a lower number of atomic displacements as the exiting ion retains a proportion of its incident energy (rather than depositing it in the target) and the collision cross-sections of the target atoms decrease with increasing ion energy. Therefore whilst it is possible to use higher energies to reduce the degree of ion implantation, a trade-off must be made with respect to the irradiation time required to achieve a given DPA level as shown in Figures 1b and 1c for the example of the time to reach 1 DPA with a typical ion flux of 10^{12} ions.cm⁻².s⁻¹.

Another consideration, beyond the total number of implanted ions or atomic displacements, is the distribution of the ions and/or damage within the TEM sample. Selection of the appropriate ion energy can be used to put helium in the middle of the foil as shown in Figure 2a for 3.3 keV helium implantation into silicon carbide or to achieve a relatively uniform distribution of damage across the sample thickness as shown in Figure 2b for 400 keV argon irradiation of tungsten. Alternatively, it may be desirable to deliberately skew a distribution within the sample. For example, graphitic materials are known to exhibit basal plane contraction under displacing irradiation with the degree of dimensional change being a function of the number of atomic displacements [28], [29]. By using 60 keV xenon ions to create an asymmetric damage profile similar to that shown in Figure 2c, it has recently been demonstrated that it is possible to induce significant strain within a sample due to the differential rates of basal plane contraction [30].

As well as species and energy, the ion beam flux is of course also a critical parameter. For many experiments the main considerations will be the required end-fluence and timescale for the irradiation. However, some experiments such as those into rate effects or single-ion phenomena may be very prescriptive as to the flux required. To take the latter example, in order to have events happen neither too often nor too infrequently it may be desirable to have a single ion arrive on average every 10 seconds in a 100×100 nm area requiring a flux of 10^9 ions.cm⁻².s⁻¹ or in a 1 μm long section of 50 nm diameter nanowire irradiated normal to its axis requiring 2×10^8 ions.cm⁻².s⁻¹.

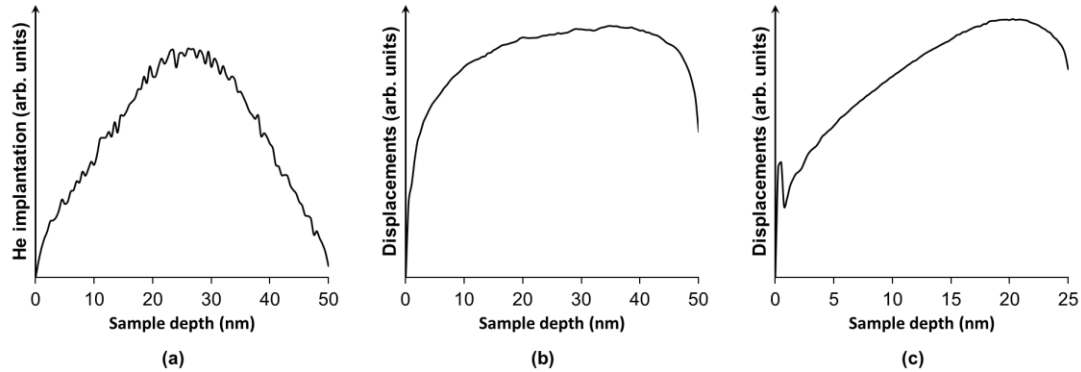


Figure 2: Results of SRIM calculations showing: (a) a peaked implantation profile for 3.3 keV helium irradiation of silicon carbide; (b) a damage profile which is relatively-flat over most of the sample depth for 400 keV argon irradiation of tungsten; and (c) a skewed damage profile for 60 keV xenon irradiation of graphite.

Rather than selecting the species and energy to control the number and of implanted ions or displaced atoms and/or their distributions, another approach to experimental design is to aim to create Primary Knock-on Atoms (PKAs) within a particular energy range so that they are, for example, below an energy threshold required to cause atomic displacement or comparable to those created by neutrons.

Simulation of neutron irradiation

Once a PKA of a given energy has been created by an atomic displacement event, the subsequent processes such as the atomic collision cascade, thermal spike phase and resulting point defect behaviour are determined only by the physical properties of the sample which is under irradiation. It does not matter whether the PKA was displaced by an electron, proton, neutron or ion. In this sense, ion beams can be used to simulate neutron irradiation directly. A typical fission neutron energy spectrum peaks at around 0.7 MeV as shown in Figure 3. At that energy, the maximum energy which can be transferred to, for example, an iron atom is about 48 keV assuming a purely-elastic binary collision. That is the same maximum energy transferable to an iron atom by a 48 keV Fe or a 50 keV Ar ion and so these, or similar, ion species and energies can be used to produce PKAs of comparable energies to those created by

neutrons in a nuclear fission reactor.

However, there are important differences between ion and neutron irradiation which should be acknowledged. Firstly, ion beams do not recreate a fission neutron energy spectrum (and therefore recoil energy spectrum) as shown in Figure 3 and can also be limited as regards the maximum energy which can be transferred to a PKA given the long high-energy tail of the neutron energy spectrum up to around 15 MeV. Secondly, the ion beams normally used in TEM with *in situ* ion irradiation do not induce nuclear transmutation events and thus phenomena such as the introduction of fission gas products are not replicated directly.

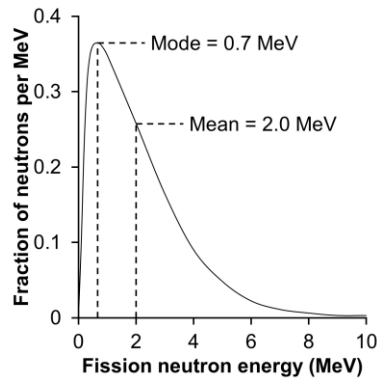


Figure 3: Energy spectrum of the prompt neutrons created by thermal fission of uranium-235.

There are several major advantages of using ion beams to simulate neutrons as compared to direct neutron irradiation. As mentioned above, the ion beams typically used in TEM with *in situ* ion irradiation do not cause nuclear transmutation events and so do not induce radioactivity in the materials under irradiation. This has clear benefits in terms of safety precautions, sample handling and instrument contamination. In addition, using heavy-inert or self-ion irradiation, in just a few hours it is possible to reach DPA levels comparable to the end-of-life for nuclear reactor core components. The cores of some Generation IV reactor designs are expected to expose structural materials to up to 200 DPA [31]. For example, using a 100 keV argon flux of 5×10^{12} ions.cm⁻².s⁻¹ it is possible to achieve 200 DPA in a 50 nm sample of iron in 3 hours, of tungsten in 2 hours or of silicon carbide in 8 hours of irradiation.

Of course, achieving such high damage levels in a few hours compared to the decades it would take in a nuclear reactor under normal operating conditions raises issues regarding dose rate effects (the interested reader is directed to chapter 11 of reference [32]). This, along with other effects such as the proximity of surfaces in a thin TEM sample, must be taken into consideration when designing and interpreting experiments with a view to understanding irradiation in nuclear environments.

Angle between the ion and electron beams

The angle, θ , between the ion and electron beams can be an important consideration in the design of *in situ* TEM facilities and experiments with smaller values of θ generally being more desirable. In order to reduce the chance of ion beam shadowing effects it can be advantageous to bring the ion beam as close as possible to the electron beam in order to avoid shadowing of the ion beam by the internal surfaces of the microscope, the TEM-sample rod and the support grid (if present) on which the sample is mounted. However, it is possible to successfully engineer around these challenges as demonstrated recently by both the JANNuS [17] and I³TEM facilities [19].

Sample sputtering is maximised when the ion beam makes an angle of about 30° to the surface at the point of incidence. Even in facilities with large values of θ , this can be ameliorated by tilting the sample towards the ion beam. An additional benefit of this is to increase the projected range of the ions into the sample which can be an advantage in situations where the maximum ion energy available is a limiting factor. However, such sample tilting can increase the effective thickness of the sample in the direction of the electron beam and thus reduce the amount of usable electron-transparent area. A requirement to tilt towards the ion beam for the aforementioned reasons can unfortunately be restricting in terms of the crystallographic orientations which are available for achieving specific electron-diffraction conditions and in terms of the sample rod geometries which can be used without blocking the electron beam. Especially for low-energy light-ion irradiation such as, for example, < 10 keV hydrogen or helium, an additional problem of large values of θ can be that the ions must traverse the strong magnetic field of the objective lens, \mathbf{B} , at angles which result in the Lorentz force deflecting them away from the sample; although with

appropriate ion beam alignment this effect may be correctable so long as large changes of objective focus (and hence changes in B) are not required during the *in situ* irradiation experiment.

However, there are some potential benefits to large values of θ even up to 90° . Firstly, the connection of the ion accelerator to the TEM can be greatly simplified by introducing the ion beam via a side port on the microscope and then through the objective pole-gap to the sample position. Due to the construction of the lower-condenser and upper-objective sections of many TEMs, it can be difficult to bring in an ion beam over the top of the objective lens without expensive and complicated modifications to the upper objective pole-piece. Secondly, there are materials systems and experiments for which irradiation normal to the electron beam is not necessarily problematic or may even be desirable. For example, the surface of nanospheres and many other nanostructures do not form a single angle with the incident ion beam thus reducing the requirement to control sputtering through sample tilting and offering the possibility of observing the effects of irradiation on the incident and exit surfaces separately.

TEM sample design and preparation

TEM sample preparation must always be performed carefully with attention paid to the nature of the experimental work for which the samples are intended. However, *in situ* TEM techniques, and in particular the combination with ion irradiation, introduce additional factors which must be considered.

For samples requiring a support grid it is essential that the grid used does not block the ion beam as illustrated in Figure 4. That said, it can sometimes be desirable to have some shadowing in order to preserve areas of a sample in the virgin state allowing direct comparison to the irradiated material after the experiment. A clear demonstration of this is shown in Figure 5a where shadowing of a silicon nanowire by its support grid has preserved a section of the nanowire and enabled a necking structure to be engineered via ion beam sputtering of the exposed material. However, if the sample requires a mesh grid and such shadowing effects are not being sought, then as large as possible mesh hole size should be used to minimise the sample area which could potentially be shadowed from the ion beam. If a choice of grid thickness is available then thinner is better so long as this does not compromise the structural integrity of

the sample and grid during the *in situ* experiment. Shadowing by the grid can often be avoided by ensuring that the sample is situated on the side of the grid on which the ion beam is incident. However, in some situations this is not possible (for example when using oyster grids which enclose the sample in a mesh on both sides) and so the selection of mesh size and suitable sample orientation within the TEM become essential.

When commencing an experiment, the next step to avoiding shadowing is to select appropriate area(s) of the sample to observe. Typically these will be regions a suitable distance from any part of the grid which could shadow the sample from the ion beam. It may also be necessary to select areas which are not only free from ion beam shadowing effects but also beyond the range of ion-beam-induced sputtering from the grid or other surfaces. These geometric considerations are illustrated in Figure 4. Finally, it should also be noted that it is not just the ion beam which can be blocked. When approaching high degrees of sample tilt to avoid ion beam shadowing effects or to establish a specific orientation for the purposes of TEM characterisation, the electron beam also has the potential to become shadowed. In these situations, mesh size, grid thickness, sample loading and area-of-interest selection are all important factors with a good understanding of the experimental geometry and construction of the TEM being essential.

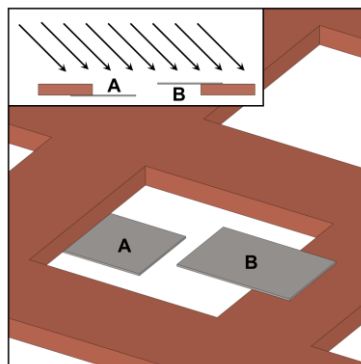


Figure 4: Schematic illustrating some geometric considerations when orientating a grid in the TEM with the ion beam incident in the direction indicated in insert. Two samples are shown mounted on a typical mesh grid with A prone to shadowing and sputtering from the grid and with B more-suitably orientated.

Similar considerations apply to the preparation and mounting of Focused Ion Beam (FIB) milled samples onto lift-out grids. In order to avoid sputtering from the grid onto the sample during the *in situ* ion irradiation, it is important to position the sample level with the grid surface on which the ion beam will be incident in the TEM. Then when loading the sample, the grid should be orientated so that the sample faces the ion beam with the grid behind it in the direction of the incident ions – similar to the orientation of sample B in Figure 4.

As well as the grid and TEM sample holder, ion beam shadowing effects can also be caused by the sample itself. For example, in the study of nanostructures such as nanowires dispersed on support films it is important that the specific structures being followed are not shadowed by their neighbours. When depositing nanostructures suspended in a solution, this can be assisted by the use of a suitably dilute mixture to reduce the areal density of the nanostructures on the grid. Other examples where self-shadowing can be problematic include crushed powders sprinkled directly on to support films or heavily-wedged samples such as those prepared by the Small Angle Cleavage Technique (SACT) [33], [34] if not properly orientated with respect to the ion beam.

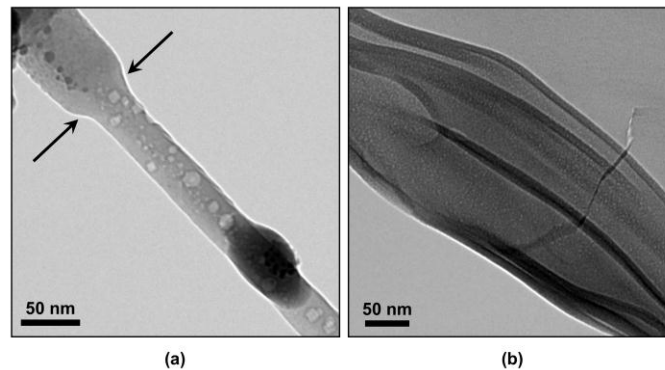


Figure 5: TEM micrographs demonstrating the effects of: (a) shadowing of a silicon nanowire under 6 keV helium irradiation at 500°C with boundary of shadowed region indicated by arrows; and (b) curling of a thin region in a silicon carbide under 3.5 keV helium irradiation at 700°C.

For *in situ* TEM experiments involving heating either intentionally through a heating holder (where heat is being supplied to the sample) or via the ion and/or electron beams themselves (where it may be necessary to remove heat from the sample), the thermal contact and conductivity between the sample, grid and sample holder should be considered. In particular, support films such as carbon or Formvar do not necessarily offer adequate thermal conduction. The thermocouple of a TEM sample holder is normally connected to the furnace in which the sample is located so the temperature reading given by the control equipment is not necessarily the same as the temperature of a particular nanoscale region of the sample at the point of observation. The best approach to address this issue is inevitably application specific and careful thought should be given if precise knowledge of the temperature is required.

TEM samples with large electron-transparent regions are often ideal for traditional imaging and characterisation. However, under *in situ* ion irradiation areas which are too thin may be prone to “curling” or “scrolling” resulting in the loss of not only those areas themselves but also of areas which they obscure as they rotate as shown in Figure 4b. This can be a particular problem in samples produced using Ion Beam Milling (IBM) preparation techniques which may feature extremely thin regions at the edges of samples. To mitigate the risk of sample curling in materials prone to this phenomenon, higher angles can be used for the final polishing stages of IBM to create a higher wedge angle featuring less of the thinnest material most likely to suffer this fate. The obvious cost of this approach is a reduced amount of electron transparent area available during the experiment. Once the sample is in the TEM, the selection of region(s) to be followed during *in situ* ion irradiation should be made so as to avoid the proximity of material likely to respond to irradiation by curling.

Preparation techniques such as IBM and FIB which use ion irradiation to produce samples can of course introduce radiation damage themselves. For *ex situ* irradiation experiments this can be a major issue as there can be ambiguity as to whether the radiation damage observed was caused exclusively by the irradiation conditions being studied and are not in some way related to the sample preparation technique. For *in situ* irradiation experiments this can be less of an issue as the regions of interest can be

characterised before, followed during and then characterised after irradiation. However, this does not mean that pre-existing radiation damage is not an issue. For example, defects may be below the resolution limit of the TEM or otherwise go undetected. The implantation of inert gases by IBM or gallium by FIB may not be immediately obvious but may influence the outcome of experiments. In situations where this is a concern, if possible it is advisable to perform additional experiments using alternative sample preparation techniques to confirm whether such effects are present.

Facilities around the world

There are currently 13 TEM with *in situ* ion irradiation facilities operating around the world as detailed in Table 1. Since the publication of the last comprehensive review of such facilities in 2009 [16], two new facilities have been established at the Ion Beam Laboratory at Sandia National Laboratories (USA) [19] and at the Centre de Recherche Public Gabriel Lippmann (Luxembourg).

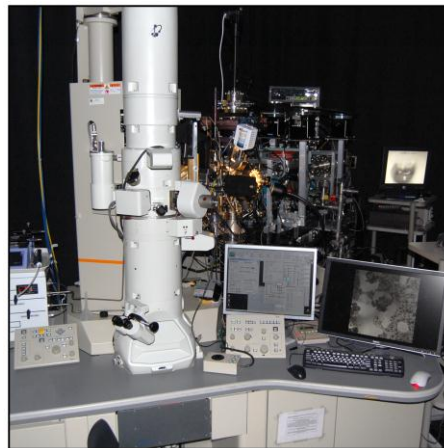


Figure 6: The recently established I^3 TEM at the Ion Beam Laboratory at Sandia National Laboratories (USA) [19] (image courtesy of K. Hattar at SNL).

The I^3 TEM facility shown in Figure 6 is located at Sandia National Laboratories (USA) consists of a JEOL JEM-2100 coupled to a 6 MV tandem accelerator and a 10 kV Colutron ion source to provide a

wide range of ion energies and species. Microfluidic and gas flow stages allow the *in situ* ion irradiation of systems such as metals undergoing corrosion opening up novel experimental possibilities not available previously in such facilities.

Another unique facility has recently been established at the Centre de Recherche Public Gabriel Lippmann (Luxembourg) and consists of an FEI Tecnai F20 fitted with a 35 kV gallium FIB [35]. Although a TEM has previously been equipped with an *in situ* FIB at NIMS [36], this new instrument is also equipped with a Secondary Ion Mass Spectrometer (SIMS) to analyse the atoms sputtered from precise regions using the FIB.

Table 1: TEMs with *in situ* ion irradiation operational in 2014.

| Facility | TEM | Ion source(s) | θ | Ref |
|--|-----------------------------|----------------------------|----------|------|
| Kyushu University (Japan) | JEOL JEM-2000EX 200 kV | 0.1–10 kV | 20° | [37] |
| Shimane University (Japan) | JEOL JEM-2010 200 kV | 1–20 kV | 17° | [38] |
| JAEA Takasaki (Japan) | JEOL JEM-4000FX 400 kV | 2–40 kV and 20–400 kV | 30° | [39] |
| JAEA Tokai-mura (Japan) | JEOL JEM-2000F 200 kV | 40 kV | 30° | [40] |
| NIMS Tsukuba (Japan) | JEOL JEM-200CX 200 kV | 5–25 kV FIB | 35° | [36] |
| NIMS Tsukuba (Japan) | JEOL JEM-ARM1000 1000 kV | 30 kV and 200 kV | 45° | [15] |
| Hokkaido University (Japan) | JEOL JEM-ARM1300 1300 kV | 20–300 kV and 20–400 kV | 44° | [16] |
| Wuhan University (China) | Hitachi H-800 200 kV | 200 kV or 3.4 MV | 90° | [41] |
| IVEM at Argonne National Laboratory (USA) | Hitachi H-9000NAR 300 kV | 650 kV or 2 MV | 30° | [14] |
| I ³ TEM at Sandia National Laboratories (USA) | JEOL JEM-2100 200 kV | 0.8–10 kV and/or 6 MV | 90° | [19] |
| JANNuS at CSNSM Orsay (France) | FEI Technai-200 200 kV | 190 kV and 2 MV | 68° | [17] |
| MIAMI at University of Huddersfield (United Kingdom) | JEOL JEM-2000FX 200 kV | 1–100 kV | 30° | [18] |
| Centre de Recherche Public, Gabriel Lippmann (Luxembourg) | FEI Tecnai F20 200 kV | 35 kV FIB | 45 | [35] |

Summary

TEM with *in situ* ion irradiation is ideally suited to studying the dynamic processes of radiation damage. It makes possible the direct observation of the microstructure during bombardment whilst also allowing experimental variables such as temperature to be controlled and maintained. Through careful sample preparation and selection of ion species, energy and flux, it is possible to tailor the experimental design to explore specific conditions and phenomena. The technique has been developing for over 50 years and there are currently 13 facilities in operation around the world. This is a field which will continue to grow to meet the challenges of developing new nuclear materials, of engineering nanostructures and of semiconductor processing as well as many other applications.

References

- [1] D. W. Pashley and A. E. B. Presland, "Ion damage to metal films inside an electron microscope," *Philos. Mag.*, vol. 6, no. 68, pp. 1003–1012, Aug. 1961.
- [2] L. M. Howe, R. W. Gilbert, and G. R. Piercy, "DIRECT OBSERVATION OF RADIATION DAMAGE PRODUCED IN COPPER BELOW 30°K DURING ION BOMBARDMENT IN THE ELECTRON MICROSCOPE," *Appl. Phys. Lett.*, vol. 3, no. 8, p. 125, 1963.
- [3] L. M. Howe and J. F. McGurn, "DIRECT OBSERVATION OF DISAPPEARANCE AND COLLAPSE OF STACKING-FAULT TETRAHEDRA IN GOLD FOILS DURING ION BOMBARDMENT IN THE ELECTRON MICROSCOPE," *Appl. Phys. Lett.*, vol. 4, no. 6, p. 99, 1964.
- [4] J. R. Parsons and L. M. Howe, "Measurement of the ion flux emanating from oxide coated emission filaments in a Siemens electron microscope," *J. Sci. Instrum.*, vol. 41, no. 12, pp. 773–775, Dec. 1964.
- [5] L. . Howe, J. . McGurn, and R. . Gilbert, "Direct observation of radiation damage produced in copper, gold and aluminum during ion bombardments at low temperatures in the electron microscope," *Acta Metall.*, vol. 14, no. 7, pp. 801–820, Jul. 1966.
- [6] P. A. Thackery, R. S. Nelson, and H. C. Sansom, "A combined heavy ion accelerator-electron microscope for the direct observation of radiation effects," Harwell, England, 1968.
- [7] P. A. Thackery and R. S. Nelson, "A combined heavy ion accelerator-electron microscope for the direct observation of radiation effects," *Proc. R. Microsc. Soc.*, vol. 4, no. 1, p. 30, 1969.

- [8] D. S. Whitmell, W. A. D. Kennedy, D. J. Mazey, and R. S. Nelson, "A heavy-ion accelerator-electron microscope link for the direct observation of ion irradiation effects," *Radiat. Eff.*, vol. 22, no. 3, pp. 163–168, Jan. 1974.
- [9] W. A. Jesser, J. A. Horton, and L. L. Scribner, "Adaptation of an ion accelerator to a high voltage electron microscope," *Radiat. Eff.*, vol. 29, no. 2, pp. 79–82, Jan. 1976.
- [10] M. O. Ruault, M. Lerme, B. Jouffrey, and J. Chaumont, "Adaptation of an ion implanter on a 100 kV electron microscope for in situ irradiation experiments," *J. Phys. E.*, vol. 11, no. 11, pp. 1125–1128, Nov. 1978.
- [11] S. Ishino, H. Kawanishi, and K. Fukuya, "In-situ observation of radiation damage by 400 keV heavy ions," *Proc. 4th Top. Meet. Technol. Control. Nucl. Fusion*, p. 1683, 1981.
- [12] A. Taylor, "In-Situ Analysis of Ion Irradiation and Implantation Effects," *IEEE Trans. Nucl. Sci.*, vol. 26, no. 1, pp. 1302–1304, Feb. 1979.
- [13] A. Taylor, J. R. Wallace, E. A. Ryan, A. Philippides, and J. R. Wrobel, "In situ implantation system in argonne national laboratory hvem-tandem facility," *Nucl. Instruments Methods Phys. Res.*, vol. 189, no. 1, pp. 211–217, Oct. 1981.
- [14] C. W. Allen, L. L. Funk, and E. A. Ryan, "New Instrumentation in Argonne's Hvem-Tandem Facility: Expanded Capability for in Situ Ion Beam Studies+," *MRS Proc.*, vol. 396, p. 641, Feb. 2011.
- [15] K. Furuya, M. Piao, N. Ishikawa, and T. Saito, "High Resolution Transmission Electron Microscopy of Defect Clusters in Aluminum During Electron and Ion Irradiation at Room Temperature," *MRS Proc.*, vol. 439, p. 331, Feb. 2011.
- [16] J. Hinks, "A review of transmission electron microscopes with in situ ion irradiation," *Nucl. Instruments Methods Phys. Res. Sect. B Beam Interact. with Mater. Atoms*, vol. 267, no. 23–24, pp. 3652–3662, Dec. 2009.
- [17] Y. Serruys, M.-O. Ruault, P. Trocellier, S. Henry, O. Kaïtasov, and P. Trouslard, "Multiple ion beam irradiation and implantation: JANNUS project," *Nucl. Instruments Methods Phys. Res. Sect. B Beam Interact. with Mater. Atoms*, vol. 240, no. 1–2, pp. 124–127, Oct. 2005.
- [18] J. A. Hinks, J. A. van den Berg, and S. E. Donnelly, "MIAMI: Microscope and ion accelerator for materials investigations," *J. Vac. Sci. Technol. A*, vol. 29, no. 2, p. 021003, 2011.
- [19] K. Hattar, D. C. Bufford, and D. L. Buller, "Concurrent in situ ion irradiation transmission electron microscope," *Nucl. Instruments Methods Phys. Res. Sect. B Beam Interact. with Mater. Atoms*, vol. 338, pp. 56–65, Nov. 2014.
- [20] S. Ishino, "Time and temperature dependence of cascade induced defect production in in situ experiments and computer simulation," *J. Nucl. Mater.*, vol. 206, no. 2–3, pp. 139–155, Nov. 1993.

- [21] S. Ishino, "A review of in situ observation of defect production with energetic heavy ions," *J. Nucl. Mater.*, vol. 251, pp. 225–236, Nov. 1997.
- [22] C. W. Allen, S. Ohnuki, and H. Takahashi, "Facilities for in situ ion beam studies in transmission electron microscopes," *Trans. Mater. Res. Soc. Japan*, vol. 17, p. 93, 1994.
- [23] C. W. Allen, "In situ ion- and electron-irradiation effects studies in transmission electron microscopes," *Ultramicroscopy*, vol. 56, no. 1–3, pp. 200–210, Nov. 1994.
- [24] C. W. Allen and E. A. Ryan, "In situ transmission electron microscopy employed for studies of effects of ion and electron irradiation on materials.," *Microsc. Res. Tech.*, vol. 42, no. 4, pp. 255–9, Aug. 1998.
- [25] R. C. Birtcher, M. A. Kirk, K. Furuya, G. R. Lumpkin, and M.-O. Ruault, "In situ Transmission Electron Microscopy Investigation of Radiation Effects," *J. Mater. Res.*, vol. 20, no. 07, pp. 1654–1683, Mar. 2011.
- [26] Y. Serruys, M.-O. Ruault, P. Trocellier, S. Miro, A. Barbu, L. Boulanger, O. Kaïtasov, S. Henry, O. Leseigneur, P. Trouslard, S. Pellegrino, and S. Vaubailon, "JANNUS: experimental validation at the scale of atomic modelling," *Comptes Rendus Phys.*, vol. 9, no. 3–4, pp. 437–444, Apr. 2008.
- [27] J. F. Ziegler, M. D. Ziegler, and J. P. Biersack, "SRIM – The stopping and range of ions in matter (2010)," *Nucl. Instrum. Meth. B*, vol. 268, no. 11–12, p. 1818, Jun. 2010.
- [28] A. J. Perks and J. H. W. Simmons, "Dimensional changes and radiation creep of graphite at very high neutron doses," *Carbon N. Y.*, vol. 4, p. 85, 1966.
- [29] R. W. Henson, A. J. Perks, and J. H. W. Simmons, "Lattice parameter and dimensional changes in graphite irradiated between 300 and 1350°C," *Carbon N. Y.*, vol. 6, no. 6, p. 789, Dec. 1968.
- [30] J. A. Hinks, S. J. Haigh, G. Greaves, F. Sweeney, C. T. Pan, R. J. Young, and S. E. Donnelly, "Dynamic microstructural evolution of graphite under displacing irradiation," *Carbon N. Y.*, vol. 68, pp. 273–284, Mar. 2014.
- [31] Y. Guérin, G. S. Was, S. J. Zinkle, and G. Editors, "Materials challenges for advanced nuclear energy systems," *MRS Bull.*, vol. 34, no. January, p. 10, 2009.
- [32] G. S. Was, *Fundamentals of Radiation Materials Science: Metals and Alloys*, 2007 ed. Springer, 2007.
- [33] J. P. McCaffrey, "Improved TEM samples of semiconductors prepared by a small-angle cleavage technique.," *Microsc. Res. Tech.*, vol. 24, no. 2, pp. 180–4, Feb. 1993.
- [34] J. P. McCaffrey, "Small-angle cleavage of semiconductors for transmission electron microscopy," *Ultramicroscopy*, vol. 38, no. 2, pp. 149–157, Nov. 1991.
- [35] T. Wirtza, D. Dowsetta, N. Vanhovea, and Y. Fleminga, "Correlative Microscopy Using SIMS For High-Sensitivity Elemental Mapping," *Microsc. Microanal.*, vol. 19 S2, p. 356, 2013.

- [36] M. Tanaka, K. Furuya, and T. Saito, "Focused Ion Beam Interfaced with a 200 keV Transmission Electron Microscope for In Situ Micropatterning on Semiconductors," *Microsc. Microanal.*, vol. 4, no. 03, pp. 207–217, Jul. 2005.
- [37] T. Muroga, R. Sakamoto, M. Fukui, N. Yoshida, and T. Tsukamoto, "In situ study of microstructural evolution in molybdenum during irradiation with low energy hydrogen ions," *J. Nucl. Mater.*, vol. 196–198, pp. 1013–1017, Dec. 1992.
- [38] K. Arakawa, T. Tsukamoto, K. Tadakuma, K. Yasuda, and K. Ono, "In-situ observation of the microstructural evolution in germanium under the low-energy helium ion irradiation," *J. Electron Microsc. (Tokyo)*, vol. 48, p. 399, 1999.
- [39] H. Abe, H. Naramoto, K. Hojou, S. Furuno, and T. Tsukamoto, "Transmission electron microscope interfaced with ion accelerators and its application to materials science," *Proc. 7th Int. Symp. Adv. Nucl. Energy Res.*, p. 365, 1996.
- [40] K. Hojou, S. Furuno, K. N. Kushita, H. Otsu, Y. Furuya, and K. Izui, "In situ EELS and TEM observation of silicon carbide irradiated with helium ions at low temperature and successively annealed," *Nucl. Instruments Methods Phys. Res. Sect. B Beam Interact. with Mater. Atoms*, vol. 116, no. 1–4, pp. 382–388, Aug. 1996.
- [41] L. P. Guo, C. S. Liu, M. Li, B. Song, M. S. Ye, D. J. Fu, and X. J. Fan, "Establishment of in situ TEM–implanter/accelerator interface facility at Wuhan University," *Nucl. Instruments Methods Phys. Res. Sect. A Accel. Spectrometers, Detect. Assoc. Equip.*, vol. 586, no. 2, pp. 143–147, Feb. 2008.